SUPPLEMENTAL MATERIAL

Inhibition of WNK3-SPAK/OSR1 kinase signaling reduces brain damage and accelerates neurological recovery after stroke

Gulnaz Begum, PhD[*], Hui Yuan, PhD[*], Kristopher T. Kahle, MD, PhD[*], Liaoliao Li, PhD, Shaoxia Wang, PhD, Yejie Shi, MD, PhD, Boris E. Shmukler, PhD, Sung-Sen Yang, MD, Shih-Hua Lin, MD, Seth L. Alper, MD, PhD, and Dandan Sun, MD, PhD[§]

SUPPLEMENTAL MATERIALS AND METHODS

MATERIALS

Antibodies that recognize A_2B_5 (R&D, Minneapolis, MN); adenomatous polyposis coli protein (APC, Millipore, Billerica, MA); microfilament associated protein-2 (MAP-2, Sigma, St Louis, MO); glial fibrillary acidic protein (GFAP, Cell Signaling, Danvers, MA); NKCC1 (T4 mAb, Developmental Studies Hybridoma Bank, Iowa City, IA); phospho-NKCC1 (p-NKCC1 $Thr^{203}/Thr^{207}/Thr^{212}$) (Cell Signaling) were previously characterized [1, 2]. Phospho-SPAK/phospho-OSR1 (p-SPAK/p-OSR1, phospho-Thr^{233}/Thr^{185}) [3]; myelin basic protein (MBP) pAb were from Chemicon International (Temecula, CA). EZ-Link™ Sulpho-NHS-SS-Biotin and NeutrAvidin® UltraLink® Resin was purchased from ThermoScientific. Mouse anti-Na^+/K^+-ATPase antibody was purchased from Developmental Studies Hybridoma Bank, Iowa City, IA. Anti-P-NKCC (R5) antibody recognizing the phosphorylated form of NKCC1/2 (p-NKCC) was the kind gift of Dr. Biff Forbush (Yale University). Fetal bovine serum (FBS) was from Valley Biomedical (Winchester, VA). Bumetanide, ciliary neurotrophic factor, poly-L-ornithine, platelet-derived growth factor (PDGF), triiodothyronine, and propidium iodide (PI) were from Sigma. Mounting medium was from Vector Laboratories (Burlingame, CA). Calcein-AM, neurobasal medium, donkey anti-sheep Alexa Fluor 488-conjugated IgG, donkey anti-mouse Alexa Fluor 546-conjugated IgG, goat anti-mouse Alexa Fluor 546-conjugated IgG, goat anti-rabbit Alexa Fluor 488-conjugated IgG, To-pro-3 iodide, Gibco B-27 supplements, Gibco glutaMAX, poly-D-lysine, and Dulbecco's Modified Eagle Medium (DMEM) were from Invitrogen (Carlsbad, CA, USA). RIPA buffer was from Pierce (Rockford, IL, USA).

METHODS

Breeding and genotyping of *WNK3* KO and *NKCC1*$^{-/-}$ mice

The gene encoding WNK3 is located on the X chromosome. Female *WNK3*$^{-/-}$(KO) mice , male *WNK3*$^{Y/-}$ (KO) mice, female *WNK3*$^{+/+}$(WT) mice, and male *WNK3*$^{Y/+}$ (WT) mice, all in the C57Bl/6J background, were obtained by a multi-step breeding scheme. First, gene-targeted *WNK3*$^{+/-}$ females and *WNK3*$^{Y/+}$(WT) males were mated to generate *WNK3*$^{Y/-}$ (KO) and *WNK3*$^{Y/+}$ (WT) males, along with *WNK3*$^{+/-}$ and *WNK*$^{+/+}$ (WT) females. Subsequent breeding mated *WNK3*$^{+/-}$ females with *WNK3*$^{Y/-}$ (KO) males, resulting in progeny including *WNK3*$^{Y/-}$ (KO) and *WNK3*$^{Y/+}$ (WT) males, along with *WNK3*$^{+/-}$ and *WNK3*$^{-/-}$ (KO) females. An additional breeding scheme to generate male *WNK3*$^{Y/-}$ (KO) males involved mating *WNK3*$^{Y/+}$(WT) males with *WNK3*$^{-/-}$ (KO) females. Mice were inbred ~16 generations at BIDMC before transfer to PITT and <3 generations of mice were used in each set of experimental results presented in this study.

P21 mice were genotyped by polymerase chain reaction (PCR) of tail DNA with a 3-primer protocol. Forward primer F1 (5'- AGGTCTTAAGAAGCTGGTGCAGG-3') amplified both wildtype (WT) and *WNK3* knockout (KO) alleles. Reverse primer R1 (5' - AAGACTGAGGAGCCAGAGAAGG-3') amplified only the WT allele. Reverse primer R2 (5'-CAGTATCGGCCTCAGGAAGATCG-3') amplified only the KO allele. Hot start PCR was performed with 35 cycles of denaturation at 94°C for 45 s, annealing at 60°C for 2 min, and extension at 72°C for 2 min. PCR products were analyzed on a 1% agarose gel, yielding a WT amplimer of 462 bp and a KO amplimer of 303 nt.

Genotyping and maintenance of the *NKCC1*$^{-/-}$ mouse colony (SV129/Black Swiss) has been described previously [4]. NKCC1 homozygous mutant and NKCC1$^{+/+}$ mice were obtained by breeding gene-targeted NKCC1 heterozygous mutant mice. The genotype of each mouse was determined by PCR of DNA from fetus tail biopsies as described [5]

Genetic analysis of *WNK3* insertional knockout (*WNK3* KO) mice

Female *WNK3*$^{-/-}$ and male *WNK3*$^{Y/-}$ knockout mice were generated from the ES cell line *RRJ530* (Bay Genomics) by the Mutant Mouse Regional Resource Centers at the University of California-Davis (mmrrc.ucdavis.edu). Genomic PCR and direct sequencing of PCR products from *WNK3* KO mice revealed insertion of the BayGenomics gene-trap vector pGT0Ixf into mouse *WNK3* Exon 4 (numbered as in human *WNK3* and as per mouse *WNK3* [**XM_909586**; corresponding to nt A111224 of BAC RP23-84O5 (**AL732420**)]. The aberrant integration included a partial vector deletion joining *WNK3* nt A111224 to vector nt C1596 (numbered from the HindIII site of pGT0Ixf). RT-PCR and direct cDNA sequencing revealed an encoded fusion protein joining WNK3 Lys258 (nt 772-774 in **XM_909586)** to His22 of the Engrailed-2 leader (nt1596-1598 in pGT0Ixf map), followed by a long ORF including the predicted full-length β-GEO reporter terminating at pGT01xf nt 5507. The vector insertion disrupts the WNK3 kinase domain, and removes the downstream WNK3 coding sequence from the predicted encoded polypeptide. The fusion protein cDNA was not sequenced in full-length.

Sequencing of mouse *WNK3* cDNA

Mouse *WNK3* cDNA from brain and kidney was PCR-amplified as overlapping cDNA fragments, purified from 1% agarose gel and sequenced. Oligonucleotide design was based on XM_909586, which described human *WNK3* as a pseudogene with ORF termination after nt 1869 (Cys 623) inside predicted exon 9. However, our direct sequencing indicated that the Exon 9 - Intron 9 boundary predicted by XM_909586 was incorrect, and that mouse *WNK3* encodes at least two full-length transcript variants (**Supplementary Figure I B**). One variant includes full-length exon 18 (JQ247189, used to derive NCBI RefSeq NM_001271678). The second variant includes a truncated exon 18 (JQ247190, used to derive NM_001271679). Both variant transcripts and the encoding genomic region lack sequence corresponding to human exon 22. Thus mouse *WNK3* exon 21 is spliced directly to exon 23, and exon 22 (per human exon nomenclature) is absent from the mouse genome.

Tissue distribution of *WNK3* transcripts

Total RNA from freshly resected mouse tissues (brain, kidney, spleen, fetal liver, liver, heart, stomach, ileum, proximal colon) and from ES cells was prepared using the RNeasy mini kit (Qiagen) or, for lung, thymus, and testis, purchased from Ambion (Austin, TX). Reverse transcription was performed with the Retroscript First Strand DNA Synthesis Kit (Ambion) using 1 μg of total RNA. 5% of this cDNA was used for Hot Start PCR (HotStarTaq DNA polymerase; Qiagen) in a total reaction volume of 50 μl in the supplier's recommended buffer. Reaction mixes were activated for 15 min at 95 °C, then subjected to 36 or 38 cycles of denaturation for 45 s at 94 °C, annealing for 2 min at 60 °C, and elongation for 2-4 min at 72 °C. Final extension of 10 min at 72 °C was terminated by rapid cooling to 4 °C. Equal volumes of PCR products were separated in 1% agarose gels for analysis, purified as necessary with the QIAquick Gel Extraction Kit (Qiagen) and sequenced. *WNK3* mRNA abundance was highest in brain, testis, and in ES cells (**Supplementary Figure I**). RT-PCR conducted with two different sets of primers yielded comparable relative abundance across all tissues tested (**Supplementary Figure I A, B**). The longer *WNK3* transcript including full-length exon 18 appeared more abundant in brain, but was detected in most other tissues as a minor band (**Supplementary Figure I**). In contrast, the transcript containing truncated exon 18 was absent from kidney, as previously noted [6]. However,

in contrast to the data of Glover et al [6], sequence corresponding to human exon 22 was absent from both *WNK3* transcripts of mouse, as well as from the mouse *WNK3* gene. The identity of all PCR amplimers was confirmed by DNA sequencing.

Middle cerebral artery occlusion (MCAO) and reperfusion

Mice were anesthetized with 3% isoflurane vaporized in N_2O and O_2 (3:2) for induction and 1.5% isoflurane for maintenance. A rubber silicon-coated monofilament suture (Filament size 6-0, diameter 0.09-0.11 mm, length 20 mm; diameter with coating 0.23 ± 0.02 mm; coating length 5 mm) was used to block MCA blood flow as previously described [7]. For reperfusion, the suture was withdrawn 60 min after MCAO. For regional cerebral blood flow (rCBF) measurement, an incision along the midline of the scalp was performed. The probe of the laser Doppler (Model PD-434, Vasa medics, LLC, St. Paul, Minnesota, USA) was placed on the intact skull (2 mm posterior and 6 mm lateral from the bregma). Tympanic membrane and rectal temperature probes were inserted and cranial and body temperatures were maintained at 36.5 ± 0.5ºC throughout the experiment by a heating blanket. For bumetanide treatment (or saline control experiments), bumetanide (10 mg/kg body weight in saline) or saline was administered via intraperitoneal (I.P.) injection, initially at 3 h reperfusion, and then daily (every 24 h) at the same dose.

Primary oligodendrocyte precursor cell (OPC) cultures

After culturing of neurospheres for 7 days, floating neurospheres were passaged at a ratio of 1:3 in the same medium every 3–4 days. To produce oligospheres, neurospheres were mechanically dissociated by 0.25% trypsin into single cell suspensions and resuspended in DMEM/F12 and 2% B27 neuronal supplement plus 10 ng/mL platelet derived growth factor (PDGF, Peprotech, Rocky Hill, NJ) and 10 ng/mL bFGF (Peprotech). After 72 h in culture, oligosphere cultures in aggregates were passaged at a ratio of 1:2 every 4–7 days. OPCs from oligospheres were generated by chemical disaggregation with 0.25% trypsin. The single OPC suspension was plated in 6- or 24-well plates (coated with 0.05% Poly-L-ornithine) at a cell density of 10^4 cells/cm^2 and OPC in DIV 2-4 were used for experiments.

Cell death assay

Cell viability was assessed by propidium iodide (PI) uptake and retention of calcein-AM as described [8]. Cultured neurons or OPCs were rinsed with the isotonic control buffer and incubated with 0.5 μM calcein-AM and 1 μg/ml PI in the same buffer at 37°C for 30 min. For cell counting, cells were rinsed with the isotonic control buffer and visualized with a Nikon TiE inverted epifluorescence microscope equipped with a Nikon 20X objective lens. Calcein-AM or PI fluorescence was visualized and cell viability expressed as the ratio of calcein-positive cells to the sum of calcein-positive and PI-positive cells.

Immunostaining image collection

40x fluorescent images were captured with a Leica DMIRE2 inverted confocal laser scanning microscope as previously described [9]. Stained cells were counted in a blinded manner by two independent researchers using ImageJ. Cells were counted in 7 evenly distributed areas (375 × 375 μm^2) in each brain section (n=4 brains) of the contralateral and ipsilateral hemispheres. Cell numbers were normalized and expressed as percentage of TO-PRO-3, MAP-2-positive, APC-positive, or GFAP-positive cells in each area. Binary image analysis was quantitated in ImageJ as described below.

Primary OPC cultures were rinsed with PBS (pH 7.4) and fixed [10]. Cells were then incubated with either primary anti-NKCC1 mAb (1:100), anti-A2B5 mAb [(1:100, a marker for precursor cells [11]], or anti-MBP pAb (1:100). Fluorescence images were captured as described above.

Binary image analysis

Binary image analysis of immunofluorescent images was conducted as described [12, 13]. Confocal images of immunofluorescence-stained brain sections (35 μm) were acquired with a Leica DMIRE2 inverted confocal laser scanning microscope, using a 40x objective, identical pinhole, intensity, and exposure parameters for all images to be compared. Background intensity in each original image was subtracted using MetaMorph image processing software, as shown in **Supplemental Figure IV A and IV B,** illustrating selection of small regions of interest (ROI, boxed areas) with minimal fluorescent signals. Background fluorescent intensities were recorded in ROIs, allowing background subtraction for each image. Note also that secondary antibody alone (Alexa-488 anti-rabbit IgG or Alexa-546 anti-mouse IgG) gave rise to minimal background fluorescence (2^{o}Ab alone, **Supplemental Figure IV**).

Binary images were generated by conversion to 8 bit images (of grayscale 0-256). These were subjected to thresholding, with pixel intensities of grayscale values 0-15 representing signals (black), and pixel intensities >15 considered as background (white). The process is illustrated in **Fig. 3 A**, in which the thresholded pSPAK/pOSR1-positive signals are black and background signals white. Specific immunoreactive signals were separated from background in each image. Changes in immnunofluorescence signals of pSPAK/pOSR1 or pNKCC1 detected in the contralateral (CL) and ipsilateral (IL) brain regions were then analyzed with ImageJ software.

In **Fig. 3A-B**, low basal levels of pSPAK/pOSR1 immunofluorescence signals were detected in soma (double **arrowhead**) in the CL hemispheres, in contrast to the high levels of overall MAP2 protein expression. However, neuronal cells in the IL peri-ischemic sections showed a sharp increase in pSPAK/pOSR1 immunoreactivity in the soma region in the binary images (**double arrowhead**). This enabled us to count neurons with increased intensity of pSPAK/pOSR1 immunoreactive signals in ischemic brain sections, then normalize those values to total TO-PRO 3^{+}-cell numbers. Because similar changes occurred in APC^{+} oligodendrocytes, the method was also applied to oligodendrocyte cell counting as shown in **Fig.3 C.**

In the case of binary images of pNKCC1 immunostaining **(Fig. 4A-C),** the CL exhibited specific signals of moderate intensity in both dendrite processes (**arrowhead**) and somata (double **arrowhead**), and ischemia increased pNKCC1 immunostaining signals differentially in these two locations. Cells with increased pNKCC1 expression in the cell body were counted and compared **(Fig. 4)**.

Luxol Fast Blue Staining

Coronal sections were stained with Luxol fast blue (American Mastertech, Lodi, CA) according to the manufacturer's protocol. The optical density of stained sections was measured from corpus callosum to external capsule in both CL and IL hemispheres using Image J software. The intensity signals in the IL were divided by those in the CL and were presented as the % optical density ratio. In striatum, the number of axonal bundles in the CL and IL was counted using Image J software. The number of axonal bundles in the IL striatum was divided by that in the CL striatum and presented as % axonal bundle ratio.

Biotinylation

Cell surface protein biotinylation labeling was performed as described previously [14]. Briefly, cultured neurons in 6-well plates were washed 2 times with PBS containing 0.5 mM $MgCl_2$ and 1 mM $CaCl_2$ (PBS-CM), then incubated with 2 ml of PBS-CM containing 1 mg/ml Sulfo-NHS-SS-Biotin (Pierce) for 30 min at 4 °C. After labeling, the biotin reaction was quenched by washing 3 times with ice-cold PBS-CM containing 50 mM glycine and 0.1% bovine serum albumin. Cells were then lysed with lysis buffer and the supernatant was collected. Protein concentration was measured with the bicinchoninic acid (BCA) assay. After correction for protein contents, 1:1 slurry of UltraLink NeutrAvidin (Pierce) was added to the supernatant (200 µg protein) to pull down the biotin-labeled surface proteins for 2 h at 4 °C. The resin bound complex was washed with PBS-CM and centrifuged for 1 min at 3000g three times. The NeutrAvidin beads were then boiled for 10 min in 2X SDS loading buffer (©Thermo Scientific Inc. (Rockford, IL) to elute biotin-labeled protein. Eluted proteins were analyzed by SDS-PAGE.

Preparation of brain membrane fractions

Mice were anesthetized with 3% isfluorane vaporized in N_2O and O_2 (3:2) and decapitated. The contralateral and ipsilateral hemispheres were dissected in five volumes of cold homogenization buffer (0.32 M sucrose, 10 mM HEPES pH 7.4, 2 mM EDTA, protease and phosphatase inhibitor cocktail (Pierce). Brain tissues were gently homogenized with a tissue pestle grinder (Kontes, Vineland, N J, USA) for 10 strokes in homogenization buffer. The homogenized samples were centrifuged at 1000 × g at 4 °C for 15 min. The supernatant (S1) was collected and centrifuged at ~200,000 x g for 30 min using Beckman Optima™ XL-80k Ultracentrifuge. The cytosolic fraction [supernatant (S2)] and crude membrane pellet were collected. The pellet was resuspended in the homogenization buffer. Protein content in both membrane and cytosolic fractions was determined by the standard BCA method.

Immunoblotting

Protein concentration in protein samples was measured with the bicinchoninic acid assay. Protein samples (20 µg cellular lysates, or 40 µg homogenates) were loaded on 7.5% sodium dodecyl sulfate gels and the proteins were electrophoretically transferred to a polyvinylidene difluoride membrane. The membrane was incubated with the rabbit anti-p-SPAK/p-OSR1 antibody (1:500 dilution) or p-NKCC1 antibody at 4°C overnight. Protein bands were visualized using enhanced chemiluminescence agents. The densities of bands were normalized to the loading control GAPDH.

SUPPLEMENTAL REFERENCES

1. Yan Y, Dempsey RJ, Flemmer A, Forbush B, Sun D. Inhibition of Na(+)-K(+)-Cl(-) cotransporter during focal cerebral ischemia decreases edema and neuronal damage. *Brain Res* 2003;961:22-31.

2. Darman RB, Forbush B. A regulatory locus of phosphorylation in the N terminus of the Na-K-Cl cotransporter, NKCC1. *J Biol Chem* 2002;277:37542-50.

3. Ohta A, Rai T, Yui N, Chiga M, Yang SS, Lin SH et al. Targeted disruption of the Wnk4 gene decreases phosphorylation of Na-Cl cotransporter, increases Na excretion and lowers blood pressure. *Hum Mol Genet* 2009;18:3978-86.

4. Flagella M, Clarke LL, Miller ML, Erway LC, Giannella RA, Andringa A et al. Mice lacking the basolateral Na-K-2Cl cotransporter have impaired epithelial chloride secretion and are profoundly deaf. *J Biol Chem* 1999;274:26946-55.

5. Su G, Kintner DB, Flagella M, Shull GE, Sun D. Astrocytes from Na(+)-K(+)-Cl(-) cotransporter-null mice exhibit absence of swelling and decrease in EAA release. *Am J Physiol Cell Physiol* 2002;282:C1147-C1160.

6. Glover M, Zuber AM, O'Shaughnessy KM. Renal and brain isoforms of WNK3 have opposite effects on NCCT expression. *J Am Soc Nephrol* 2009;20:1314-22.

7. Luo J, Wang Y, Chen H, Kintner DB, Cramer SW, Gerdts JK et al. A concerted role of Na(+)-K(+)-Cl(-) cotransporter and Na(+)/Ca(2+) exchanger in ischemic damage. *J Cereb Blood Flow Metab* 2008;28:737-46.

8. Beck J, Lenart B, Kintner DB, Sun D. Na-K-Cl cotransporter contributes to glutamate-mediated excitotoxicity. *J Neurosci* 2003;23:5061-8.

9. Shi Y, Chanana V, Watters JJ, Ferrazzano P, Sun D. Role of sodium/hydrogen exchanger isoform 1 in microglial activation and proinflammatory responses in ischemic brains. *J Neurochem* 2011;119:124-35.

10. Chen H, Kintner DB, Jones M, Matsuda T, Baba A, Kiedrowski L et al. AMPA-mediated excitotoxicity in oligodendrocytes: role for Na(+)-K(+)-Cl(-) co-transport and reversal of Na(+)/Ca(2+) exchanger. *J Neurochem* 2007;102:1783-95.

11. O'Donnell ME, Lam TI, Tran L, Anderson SE. The role of the blood-brain barrier Na-K-2Cl cotransporter in stroke. *Adv Exp Med Biol* 2004;559:67-75.

12. Morrison HW, Filosa JA. A quantitative spatiotemporal analysis of microglia morphology during ischemic stroke and reperfusion. *J Neuroinflammation* 2013;10:4.

13. Jen KY, Nguyen TB, Vincenti FG, Laszik ZG. C4d/CD34 double-immunofluorescence staining of renal allograft biopsies for assessing peritubular capillary C4d positivity. *Mod Pathol* 2012;25:434-8.

14. Lee HH, Jurd R, Moss SJ. Tyrosine phosphorylation regulates the membrane trafficking of the potassium chloride co-transporter KCC2. *Mol Cell Neurosci* 2010;45:173-9.

15. Vitari AC, Thastrup J, Rafiqi FH, Deak M, Morrice NA, Karlsson HK et al. Functional interactions of the SPAK/OSR1 kinases with their upstream activator WNK1 and downstream substrate NKCC1. *Biochem J* 2006;397:223-31.

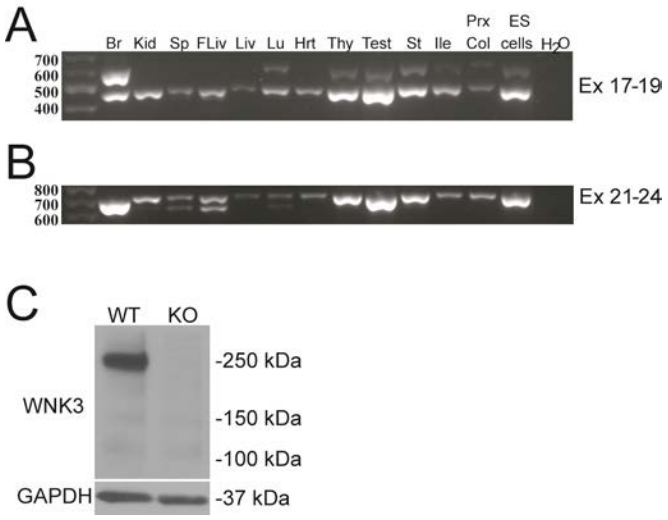

Figure I. WNK3 tissue distribution in mouse

A-**B**. Tissue distribution of mouse *WNK3* mRNA. Mouse tissue cDNAs were subjected to 38 cycles PCR (36 cycles for brain, testis, ES cells) with (in panel A) exon 17 forward primer 17F (5'-ACCTGCTCTATCAGGAGCACAG-3') and exon 19 reverse primer 19R (5'-CCCTAGTATCAGATGAGAACTCC-3'), and (in panel B) exon 21 forward primer "20"F (5'-CTTTGTCACCTGCATCGCCACG-3') and exon 24 (3'-UTR) reverse primer 3R2 (5'-GTGTAGCATCACAGGTGTTCTG-3'); exon numbering is as per the human *WNK3* gene. Direct sequencing of cDNA amplimers from panel A revealed two alternate splice patterns for exon 18: the upper band of panel A contains full-length exon 18, whereas the lower band has a 141 bp (47 codon) in-frame deletion/truncation of the 3'-end of exon 18. Direct sequencing of major cDNA bands from panel B (including brain) showed that mouse *WNK3* exon 21 is directly spliced to exon 23 in *WNK3* mRNA. DNA sequence homologous to human exon 22 was absent from the mouse genome (not shown). The lower band in panel B (visible in spleen, fetal lever and lung) was shown by direct sequencing to be nonspecific and unrelated to Wnk3. Leftmost lane, molecular size markers; Br, brain; Kid, kidney; Sp, spleen; FLiv, fetal liver; Liv, liver; Lu, lung; Hrt, heart; Thy, thymus; Test, testis; St, stomach; Ile, ileum; Prx Col, proximal colon. The rightmost lane (H_2O) is a noncontiguous negative control lane from the same gel.

C. Representative Western blot of brain lysates harvested from *WNK3* WT and *WNK3* KO, subjected to SDS-PAGE, and probed with a specific anti-WNK3 antibody [15].

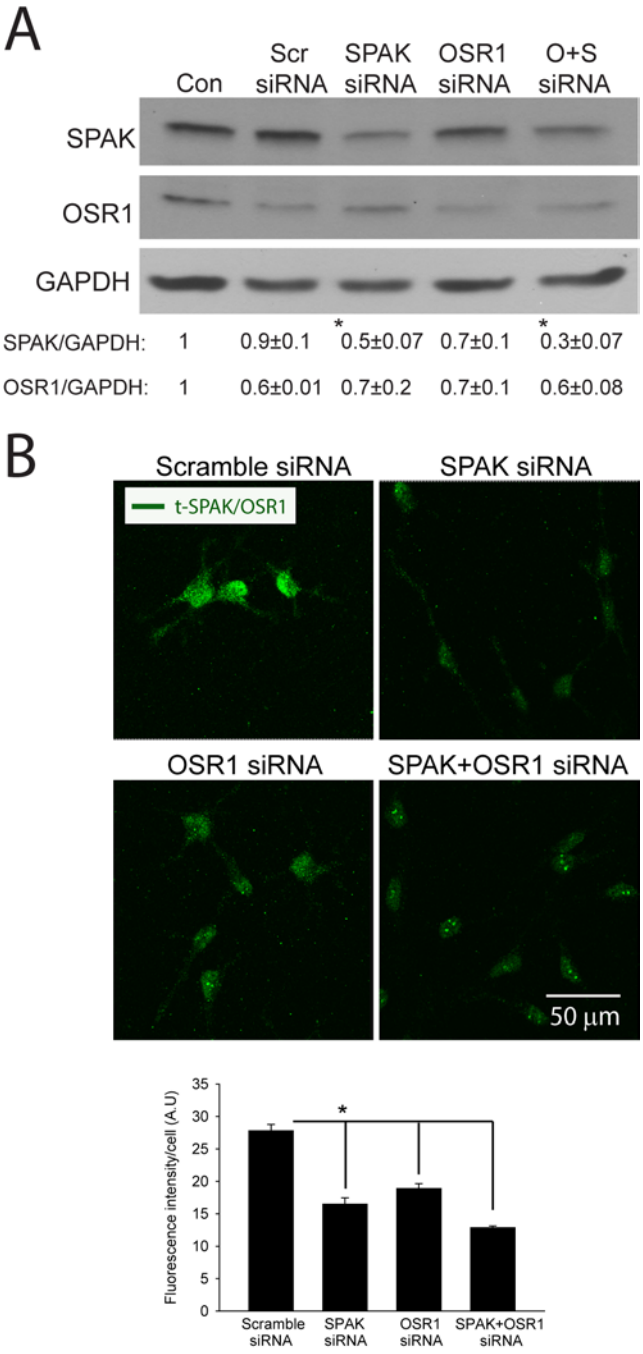

Figure II. SiRNA-mediated knockdown of SPAK/OSR1 protein expression

A. Representative immunoblots showing siRNA-induced knockdown of SPAK/OSR1 protein expression in neurons. Cortical neurons were treated for 72 h with control medium, scrambled siRNA (Scr), SPAK siRNA, OSR1 siRNA, or both (O+S). The level of SPAK/OSR1 protein expression was determined and normalized to loading control protein. Relative expression level of SPAK and OSR1 in each group was then normalized to the control group. Numerical data are means ± SEM. n = 5. * $p < 0.05$ vs. Scr.

B. Representative immunostaining images showing siRNA-induced knockdown of SPAK/OSR1 protein expression in OPCs using a protocol similar to that of panel A. Data are means ± SEM. n = 3. * $p < 0.05$ vs. Scr.

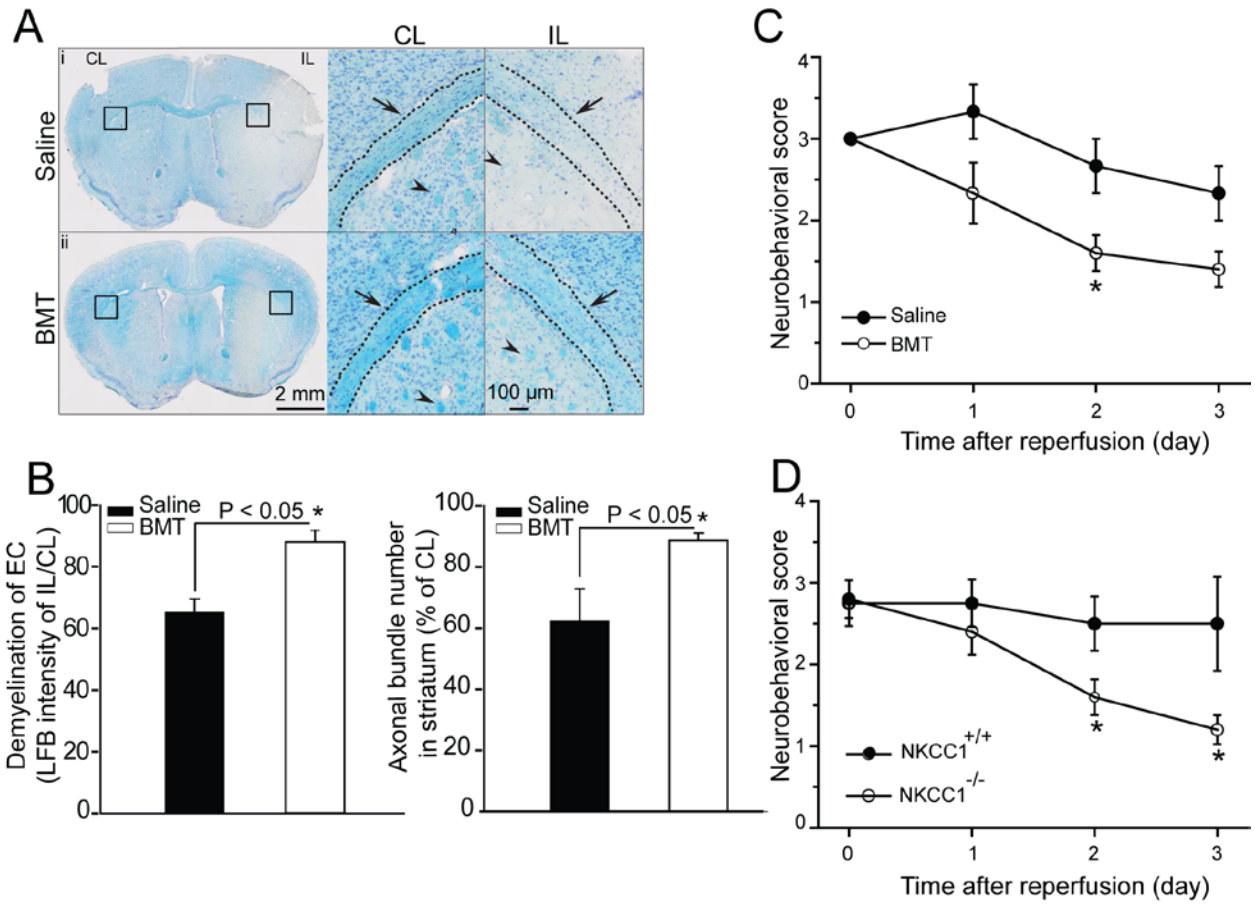

Figure III. Reduction in white matter injury in WT mice treated with NKCC1 inhibitor bumetanide (BMT).

A. Left panel: Bright field images of saline- (i) or BMT-treated WT mouse brain sections (ii) stained with LFB and cresyl violet at 3 day after MCAO. BMT (10 mg/kg) was injected intraperitoneally at 3, 24 and 48 h Rp. Saline was used as a vehicle control. *Black boxes*: regions in which external capsule demyelination of white matter were measured in the CL and IL hemispheres. Right panel: higher magnification images. *Arrowhead*: myelinated or demyelinated axonal bundles. *Arrow*: Axonal track. **B**. Summary of demyelination data. Values represent Mean ± SD (n = 3). *p < 0.05 *vs.* saline. **C-D**. Improved neurological behavior in either BMT-treated WT mice or *NKCC1*$^{-/-}$ mice after MCAO. Values represent mean ± SD (n=3). *P < 0.05 vs. Con or WT.

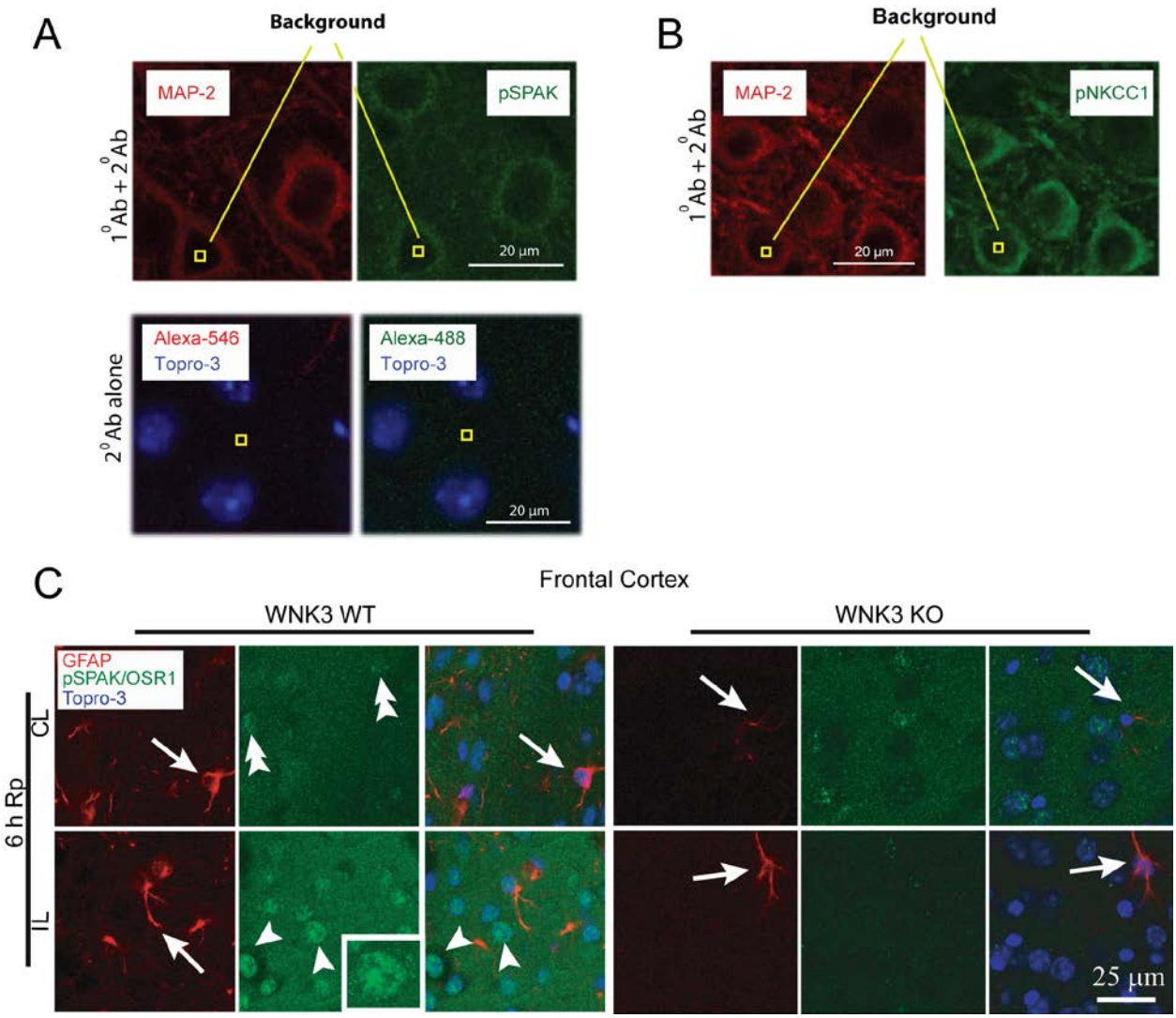

Figure IV. Image analysis and lack of pSPAK/pOSR1 expression in GFAP$^+$ cells in early reperfusion

A-B. Images illustrate representative areas selected for background intensity assignment for background subtraction prior to binary image analysis.

C. Representative images of pSPAK/pOSR1 (*green*), the glial marker GFAP (*red*), or nuclear To-pro-3 (*blue*) staining in the CL and IL of wild-type (WT) or *WNK3* knockout (KO) mice were shown at 6 h Rp after MCAO as described in *Methods*. **Insets:** magnified images. ***Arrow:*** astrocytes. ***Double Arrowhead***: basal level of pSPAK/pOSR1 expression; ***Arrowhead***: increased expression of pSPAK/pOSR1. *Scale bar*: 25 µm.

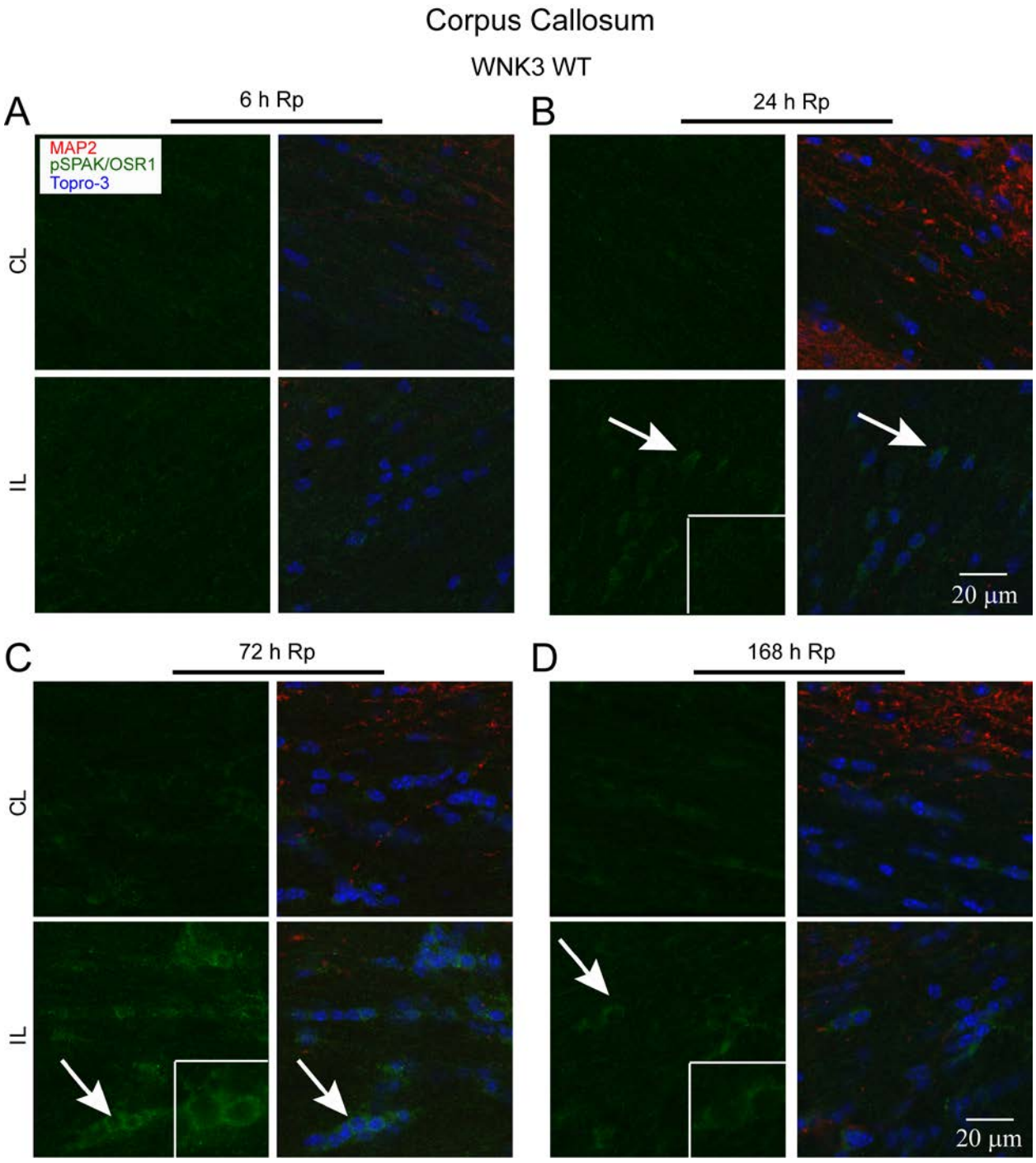

Figure V. Time-dependent expression of pSPAK/pOSR1 in the corpus callosum after cerebral ischemia

A-D. Representative images of pSPAK/pOSR1 (*green*), neuronal marker MAP2 (*red*), or nuclear To-pro-3 (*blue*) staining in the corpus callosum in the CL and IL of wild-type (WT) mice were shown at 6, 24, 72, or 168 h Rp after MCAO as described in *Methods*. **Insets:** magnified images. ***Arrow:*** increased expression of pSPAK/pOSR1. *Scale bar*: 20 μm.